TO APPEAR IN THE ASTRONOMICAL JOURNAL
Preprint typeset using LaTeX style emulateapj v. 04/03/99



# RR LYRAE STARS IN THE ANDROMEDA HALO FROM DEEP IMAGING WITH THE ADVANCED CAMERA FOR SURVEYS[1]

THOMAS M. BROWN, HENRY C. FERGUSON, ED SMITH
Space Telescope Science Institute, 3700 San Martin Drive, Baltimore, MD 21218; tbrown@stsci.edu, ferguson@stsci.edu, edsmith@stsci.edu
RANDY A. KIMBLE, ALLEN V. SWEIGART
Code 681, NASA Goddard Space Flight Center, Greenbelt, MD 20771; randy.a.kimble@nasa.gov, allen.v.sweigart@nasa.gov
ALVIO RENZINI
European Southern Observatory, Karl-Schwarzschild-Strasse 2, Garching bei München, Germany; arenzini@eso.org
R. MICHAEL RICH
Division of Astronomy, Dpt. of Physics & Astronomy, UCLA, Los Angeles, CA 90095; rmr@astro.ucla.edu

*To appear in The Astronomical Journal*

## ABSTRACT

We present a complete census of RR Lyrae stars in a halo field of the Andromeda galaxy. These deep observations, taken as part of a program to measure the star formation history in the halo, spanned a period of 41 days with sampling on a variety of time scales, enabling the identification of short and long period variables. Although the long period variables cannot be fully characterized within the time span of this program, the enormous advance in sensitivity provided by the Advanced Camera for Surveys on the Hubble Space Telescope allows accurate characterization of the RR Lyrae population in this field. We find 29 RRab stars with a mean period of 0.594 days, 25 RRc stars with a mean period of 0.316 days, and 1 RRd star with a fundamental period of 0.473 days and a first overtone period of 0.353 days. These 55 RR Lyrae stars imply a specific frequency $S_{RR} \approx 5.6$, which is large given the high mean metallicity of the halo, but not surprising given that these stars arise from the old, metal-poor tail of the distribution. This old population in the Andromeda halo cannot be clearly placed into one of the Oosterhoff types: the ratio of RRc/RRabc stars is within the range seen in Oosterhoff II globular clusters, the mean RRab period is in the gap between Oosterhoff types, and the mean RRc period is in the range seen in Oosterhoff I globular clusters. The periods of these RR Lyraes suggest a mean metallicity of [Fe/H]$\approx -1.6$, while their brightness implies a distance modulus to Andromeda of $24.5 \pm 0.1$, in good agreement with the Cepheid distance.

*Subject headings:* galaxies: evolution – galaxies: stellar content – galaxies: halos – galaxies: individual (M31) – stars: variables

## 1. INTRODUCTION

The textbook picture of a spiral galaxy halo comes from that of our own Milky Way, which is old and metal-poor (Vanden-Berg 2000; Ryan & Norris 1991). However, the stellar population of the Andromeda (M31; NGC224) halo offers a striking contrast to this picture, with its wide range in metallicity (Durrell, Harris, & Pritchet 2001) and age (Brown et al. 2003; Brown 2003). These spreads in metallicity and age can significantly affect the variable star population. For example, the characteristics of RR Lyraes in Galactic globular clusters place these clusters into two distinct Oosterhoff types (Oosterhoff 1939), while the RR Lyraes in Local Group dwarf spheroidals (dSphs) place these galaxies in the gap between the two Oosterhoff types (Siegel & Majewski 2000; Dall'Ora et al. 2003; Pritzl et al. 2002, 2004). Compared to the M31 halo, dSphs have an even broader age range (van den Bergh 1999) and are generally more metal-poor (Mateo 1998), but the old ($>10$ Gyr) component capable of producing RR Lyrae stars might be similar in each case.

The specific frequency of RR Lyraes in the M31 halo has been the subject of some debate. In a field 40 arcmin from the nucleus on the southeast minor axis, Pritchet & van den Bergh (1987) found 30 RR Lyraes, and with an estimated completeness of 25%, determined that the frequency per unit luminosity was very high (about half of that in variable-rich M3). More recently, Dolphin et al. (2003) found only 24 RR Lyraes in a larger field that included the Pritchet & van den Bergh (1987) field, and with their estimated completeness of 24%, claimed that the frequency of RR Lyrae was $\sim$15 times smaller. To support their claim, they estimated that the deep color magnitude diagram (CMD) of Brown et al. (2003) contained only 10 RR Lyraes, but as we shall show here, this was a severe underestimate.

We have observed a field along the southeast minor axis of the M31 halo, 51 arcmin from the nucleus, using the Advanced Camera for Surveys (ACS; Ford et al. 1998) on the Hubble Space Telescope (HST). The primary goal of this program was to investigate the halo star formation history, by constructing a deep CMD in the F606W (broad $V$) and F814W ($I$) bandpasses, reaching $V \approx 30.7$ mag on the main sequence (Brown et al. 2003). However, the 250 individual exposures are scattered with variable time sampling over a 41 day period, and thus provide excellent time series photometry for the variable star population in the M31 halo; in particular, the completeness for RR Lyraes in our field is approximately 100%. In this paper, we present a survey of the RR Lyraes and the other bright variables in our field.

[1]Based on observations made with the NASA/ESA Hubble Space Telescope, obtained at the Space Telescope Science Institute, which is operated by AURA, Inc., under NASA contract NAS 5-26555. These observations are associated with proposal 9453.

## 2. OBSERVATIONS AND DATA REDUCTION

Using the Wide Field Camera on the ACS, we obtained deep optical images of a $3.5' \times 3.7'$ field along the southeast minor axis of the M31 halo, at $\alpha_{2000} = 00^h46^m07^s$, $\delta_{2000} = 40^o42'34''$. The surface brightness in this region is $\mu_V \approx 26.3$ mag arcsec$^{-2}$ (Brown et al. 2003). The area is not associated with the tidal streams and substructure found by Ferguson et al. (2002), and lies just outside the "flattened inner halo" in their maps. We placed a metal-rich M31 globular cluster, GC312 (Sargent et al. 1977), near the edge of the field. From 2 Dec 2002 to 11 Jan 2003, we obtained 39.1 hours of images in the F606W filter (broad $V$) and 45.4 hours in the F814W filter ($I$), with each of the 250 exposures dithered to allow for hot pixel removal, optimal point spread function sampling, smoothing of spatial variations in detector response, and filling in the gap between the two halves of the $4096 \times 4096$ pixel detector. Of the 250 exposures, 16 were short ($< 600$ s), to allow the correction of bright saturated objects, leaving 234 long exposures ($> 1200$ s) suitable for deep time-series photometry.

In order to create a deep catalog of the objects in this field, we first co-added these images using the IRAF DRIZZLE package. This coaddition included masks for the cosmic rays and hot pixels, and produced geometrically-correct images with a plate scale of $0.03''$ pixel$^{-1}$ and an area of approximately $210'' \times 220''$. The mask for each exposure was created in an iterative process, comparing the value in every pixel to the distribution through the entire stack at that location on the sky; pixels are masked on the bright end of the distribution (cosmic rays and hot pixels) and the faint end of the distribution (dead pixels), but this technique also masks bright, large-amplitude, variable stars when they are near maximum or minimum. The final coadded image in each bandpass thus approximates the average flux observed for the variable stars, but these masks cannot be used in the time series photometry (discussed below).

We then performed both aperture and PSF-fitting photometry using the DAOPHOT-II package (Stetson 1987), assuming a variable PSF constructed from the most isolated stars. The aperture photometry on isolated stars was corrected to true apparent magnitudes using TinyTim models of the HST PSF (Krist 1995) and observations of the standard star EGGR 102 (a $V = 12.8$ mag DA white dwarf) in the same filters, with agreement at the 1% level. The PSF-fitting photometry was then compared to the corrected aperture photometry, in order to derive the offset between the PSF-fitting photometry and true apparent magnitudes. Our photometry is in the STMAG system: $m = -2.5\times \log_{10} f_\lambda - 21.1$. For readers more familiar with the Johnson $V$ and Cousins $I$ bandpasses, a star in the middle of the RR Lyrae strip has $V - m_{F606W} = -0.17$ mag and $I - m_{F814W} = -1.29$ mag. Light curve amplitudes are typically 6–10% smaller in $m_{F606W}$ than in $V$, and 1–2% smaller in $m_{F814W}$ than in $I$. The transformation between the ACS and ground-based bandpasses is still being characterized independently by several groups, so for most of this paper we will refer to magnitudes in the unambiguous STMAG system.

The CMD for the co-added images was shown by Brown et al. (2003). In that analysis, we discarded ≈20% of the exposed area (around bright foreground stars, near GC312, and in regions with less than the full exposure time due to the dither pattern). In the current analysis of the brighter stars, we include the entire image area. We will only consider stars brighter than $m_{F814W} = 28.25$ mag, which have a signal-to-noise ratio of $\sim 5$ in individual exposures. Extensive artificial star tests demonstrate that our catalog, created from the deep co-added data, is ≈100% complete above this limit.

To obtain time-series photometry, we re-drizzled the entire dataset into a stack of individual registered exposures, with masked pixels set to an invalid data value. Because our original masks sometimes discard data points near the maxima and minima of variable stars, we unmasked those pixels that were masked more than once in a two-hour window; this correction will occasionally restore a true cosmic ray or dead pixel when it should have been masked, but these occasional events will be significant outliers in the time series photometry, which can be discarded after the fact. We then performed aperture photometry on each individual frame, with positions fixed by the catalog of the coadded exposures.

## 3. VARIABLE DETECTION AND CHARACTERIZATION

As explained above, we restricted our time-series analysis to stars brighter than $m_{F814W} = 28.25$ mag; out of the nearly 300,000 stars in the full image catalog, these 19,450 stars have a signal-to-noise of at least 5 in individual exposures. Stars in the RR Lyrae gap, near $m_{F814W} \approx 26$ mag, have typical photometric errors of 0.03 mag in F606W exposures and 0.04 mag in F814W exposures. Most of the stars in our search list have $\sim 100$ photometric measurements in each bandpass over our 41 day observing program, but a small fraction have significantly less because they fell near the edges of the two halves of the detector; 424 stars, representing only 2% of the stars in the relevant brightness range, were discarded because they had less than 30 valid measurements in each bandpass. For the remaining stars, we looked for variability using two methods, chosen to suit the high signal-to-noise and large number of time samples in these data.

The first variability search was tuned to provide a complete sample of RR Lyraes, but it also recovered a large number of brighter, long period variables and fainter, short period variables. We used a fast algorithm (Press & Rybicki 1989) of the Lomb-Scargle periodogram (Lomb 1976; Scargle 1982), which looks for weak periodic signals in irregularly sampled data. Besides providing a good initial estimate of the period, this algorithm also quantifies the statistical significance of the periodic signal. Our threshold was a non-random signal at 0.01 significance, independently found in each bandpass; a score of 0.01 implies that the chance this signal arose from random fluctuations is less than 1 percent. This stringent threshold should only produce one or two false detections in the entire search list. However, this threshold is not so stringent that it misses RR Lyraes; all of the RR Lyraes recovered by this method, regardless of amplitude or period, were detected at a significance orders of magnitude beyond this threshold (if our choice of threshold were in fact discarding RR Lyraes, then the distribution of RR Lyrae scores would approach the threshold). The initial period estimate returned by this method was then refined by a search of the Lafler & Kinman (1965) statistic, for periods within 5% of the initial period. Our method recovered 169 variables, two of which were false detections (each a faint star sitting in the wings of a bright variable), and 55 of which are clearly RR Lyraes. Of the remaining variables, 17 are short period variables below the horizontal branch (HB), 3 have periods of 0.6–7 days and lie above the HB, 1 is an eclipsing binary, 82 are long period variables (LPVs) and semiregulars near the tip of the red giant branch (RGB), 5 are LPVs fainter than the HB, and 4 are variables with periods of $\sim$1 week that lie on the RGB. Thirteen of the detected variables, all with periods

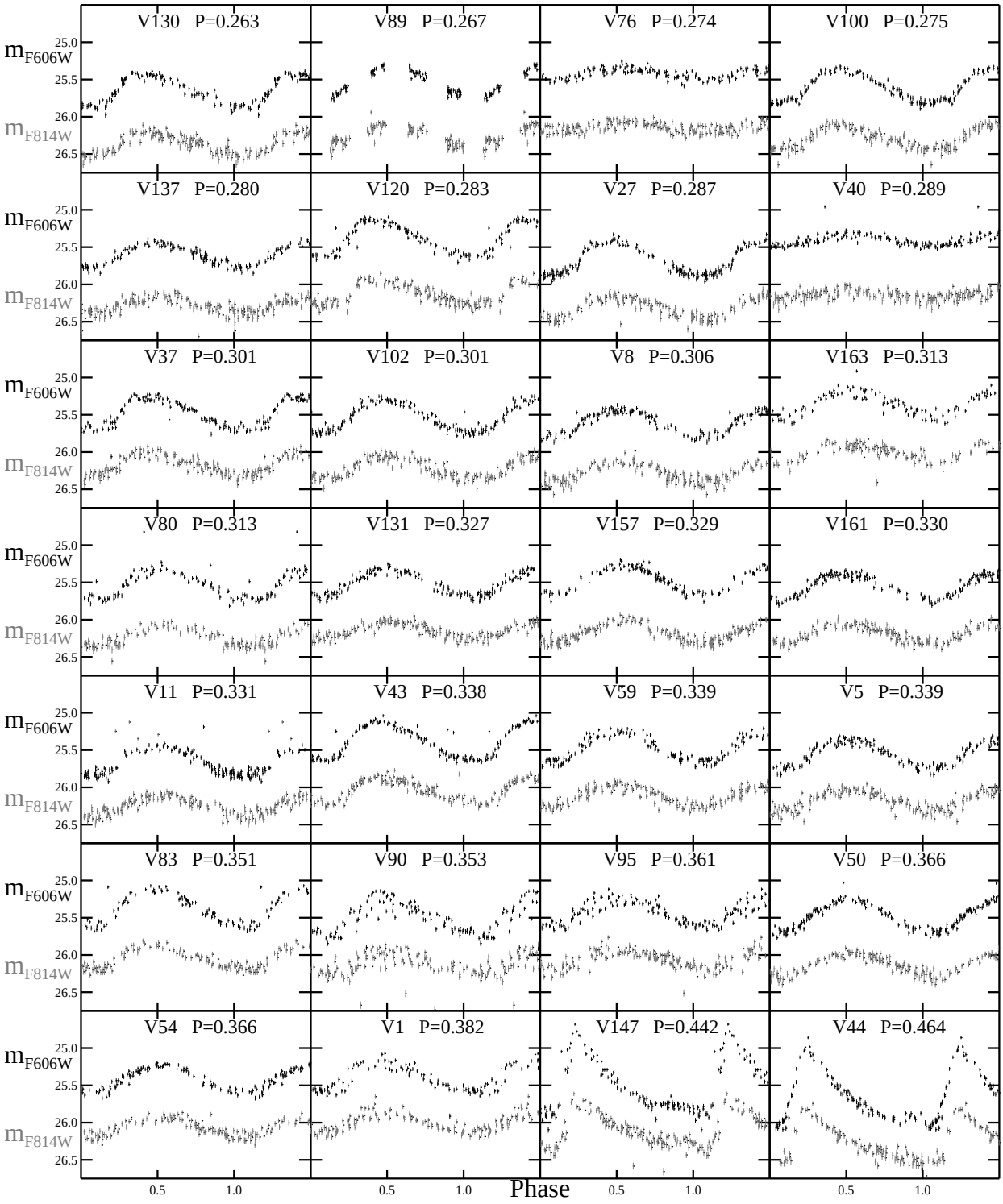


FIG. 1– The light curves for RR Lyraes in our field, arranged in order of increasing period (*labeled*), shown as photometric error bars (not data points). The first 26 stars are RRc and RRd stars (V90 being the RRd, shown phased with its first overtone period); the remaining 29 are RRab stars.

longer than 20 days, fall within the tidal radius of GC312 (10″; Holland et al. 1997); because the area within the tidal radius of GC312 comprises less than 1 percent of our total field, these 13 LPVs and semiregulars are clearly associated with GC312.

The second variability search simply looked for photometry that exceeded the expected scatter (given the photometric errors) by 50%. This method was motivated by a search for halo-on-halo microlensing events. We found no microlensing events or new pulsating variables, but we did find 7 additional eclipsing binaries. As might be expected, the Lomb-Scargle periodogram is better suited to finding variables with roughly sinusoidal light curves. We show the light curves for the RR

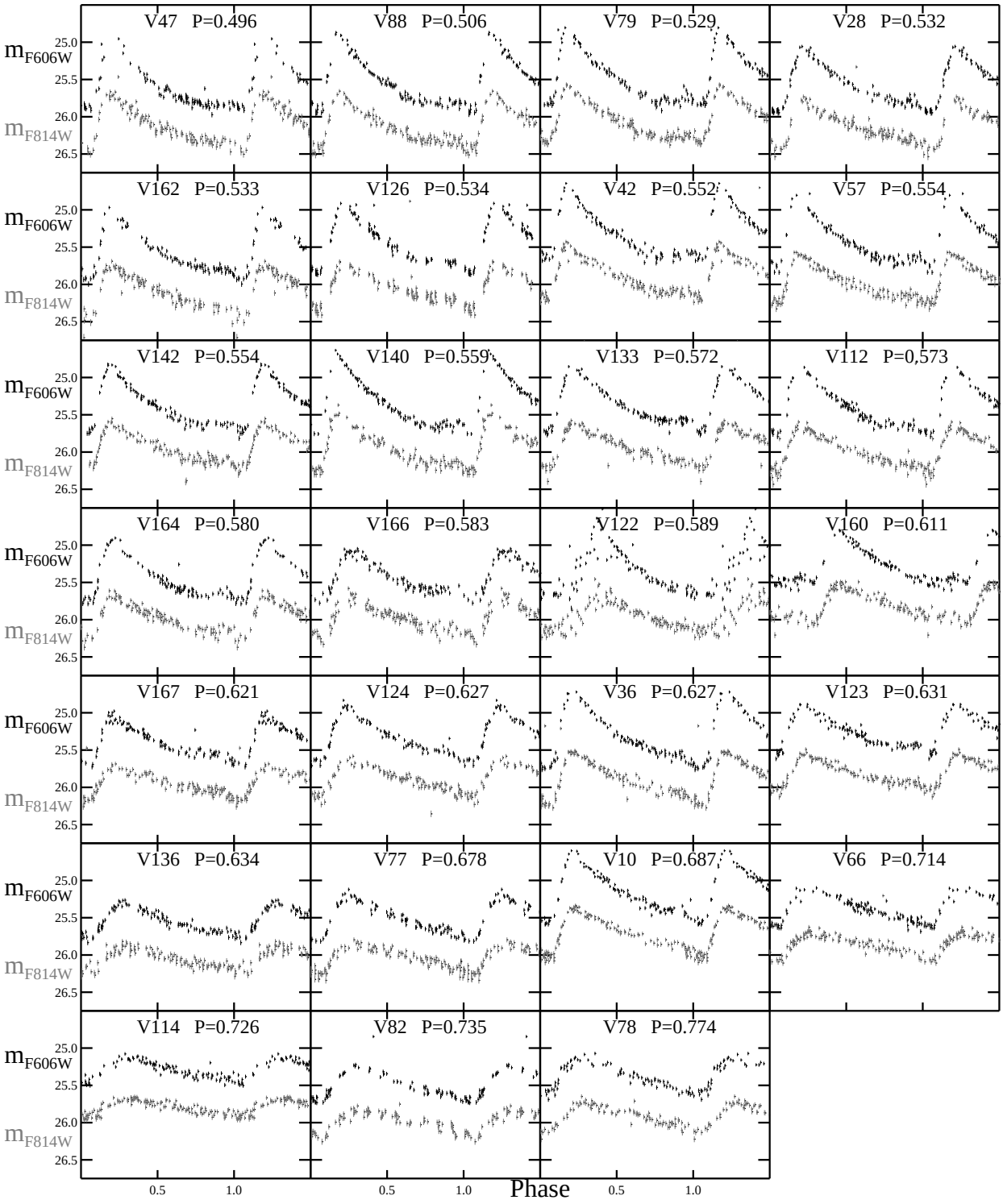


FIG. 1– Continued.

Lyraes in Figure 1, light curves for the variables above and below the HB in Figure 2, light curves for the eclipsing binaries in Figure 3, and light curves for a subset of the LPVs and semiregulars in Figure 4 (only those that varied by more than $\sim 0.1$ mag within the 41 days of observations). Note that only photometric error bars are visible at the plotted scale of these light curves.

Five of the RR Lyrae light curves show significant scatter (V1, V90, V95, V122, and V163). We reevaluated the periodicity searches on these five stars, and found that one of the stars, V90, showed clear evidence for double-mode pulsations, making it a definite RRd star, with a fundamental period ($P_0$) of 0.4735 days and a first overtone period ($P_1$) of 0.3534 days. V163 shows a hint of an additional period at 0.4243 days, but the signal is weak, and we found no additional periods

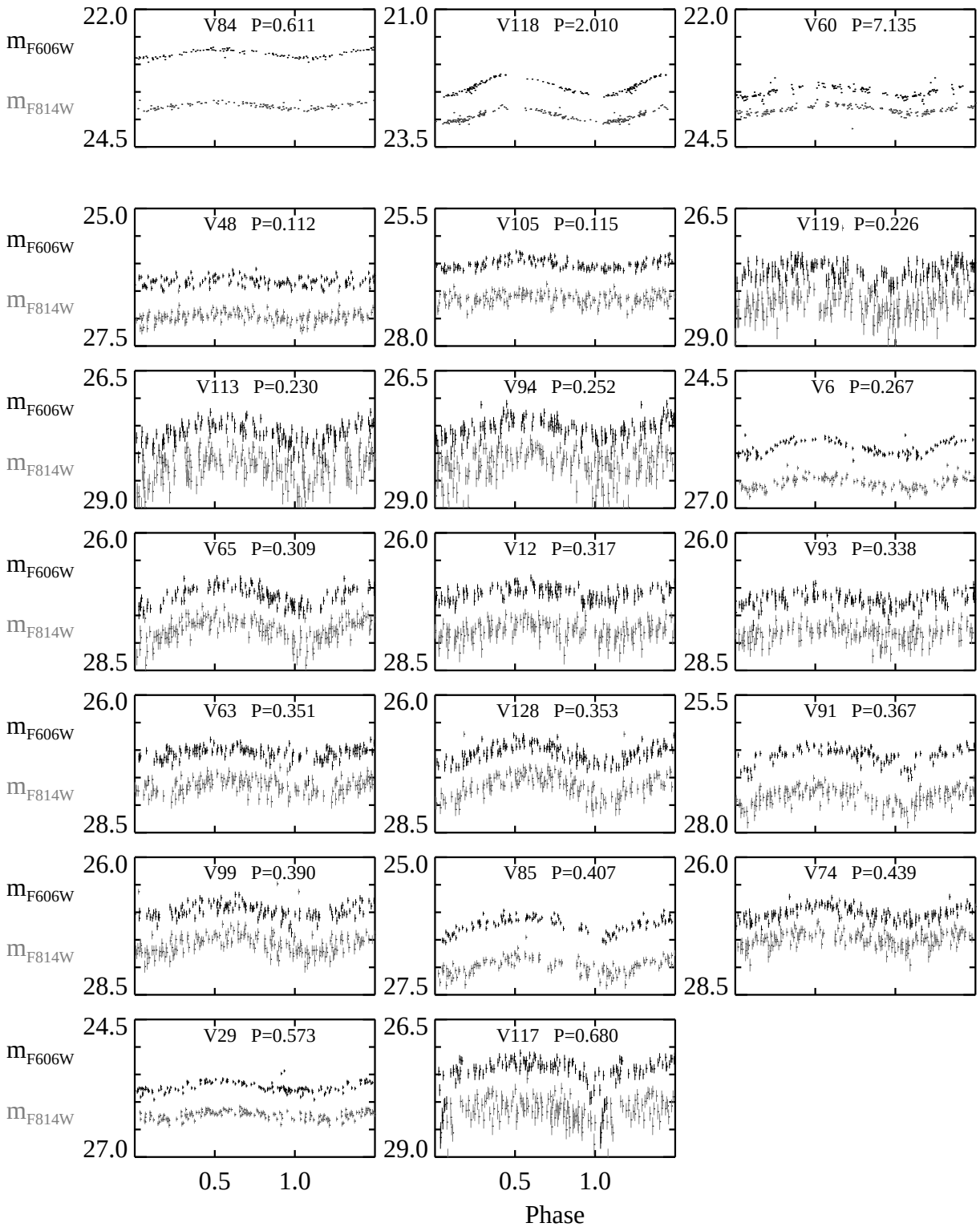


FIG. 2– The light curves for other variables bluer than the RGB (excluding eclipsing binaries), shown as error bars. The stars in the top 3 panels are brighter than the HB; they are arranged in order of increasing period and increasing $m_{F606W} - m_{F814W}$ color, making them easy to identify in the CMD (Figure 5). The stars in the lower 17 panels are likely dwarf Cepheids fainter than the HB, but V6 and V29, which lie immediately below the HB, might be RR Lyraes.

in the light curves of V1 and V95. Although V1, V95, and V163 might be RRd stars, we have classified them as RRc. The scatter in the light curve of V122 might be due to the Blazhko effect – a secondary modulation in the variability of 20–30% of RRab stars, with a period of ∼10–500 days (Smith et al. 2003).

To determine the mean magnitudes and amplitudes of the variables with periods less than ∼ 10 days, we fit a Fourier series to the magnitudes in each bandpass as a function of phase, with an order of 1 or 2 for the sinusoidal light curves (e.g., RRcd stars) and an order of 8 for the sawtooth light curves (e.g.,

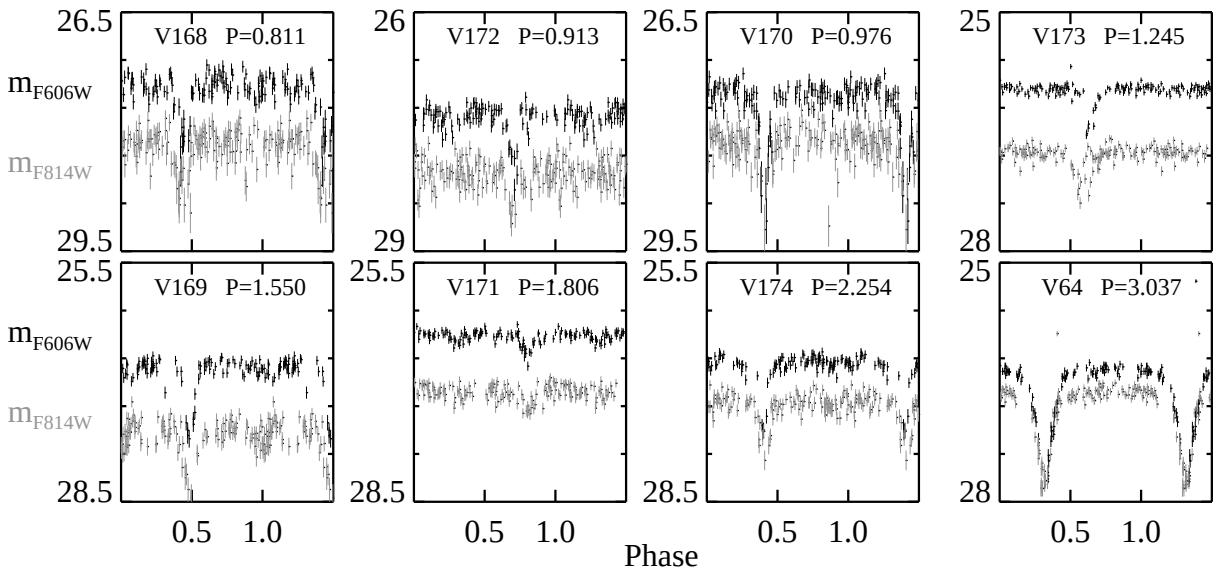


FIG. 3– The light curves for candidate eclipsing binaries in our field. The most secure (V64) was found through the Lomb-Scargle periodogram search, while the others were found because their photometric errors were larger than expected. Note that a secondary minimum is sometimes visible at a phase opposite to the primary minimum.

RRab stars). Table 1 lists the properties of the RR Lyraes in our field, and Table 2 gives their time-series photometry (with the full dataset available only as a machine-readable table in the electronic version of this paper). Table 3 gives the positions of the other variables in our field (Figures 2–4). Figure 5 shows the CMD locations of the stars with light curves (Figures 1–4). The variables are shown at their mean $m_{F606W} - m_{F814W}$ color and $m_{F814W}$ magnitude, as determined from the fitting above, instead of the average *observed* value in the catalog from the deep co-added images, which can be systematically brighter or fainter in a given bandpass by a few hundredths of a magnitude, depending upon the random sampling of each light curve. Figure 6 shows the distribution of $m_{F606W}$ amplitude vs. period, mean $m_{F606W}$ vs. period, and the period distribution for the RR Lyrae stars. The RR Lyraes are cleanly separated from the remaining variables by their position in the $m_{F606W}$ vs. period diagram, although two stars lying immediately below the HB might also be RR Lyraes (V6 and V29 in Figure 2). The RR Lyraes can be classified as either RRab or RRcd by the gap in amplitude vs. period distribution; these classes do not overlap in the CMD (Figure 5).

## 4. RR LYRAE PROPERTIES

### 4.1. *Oosterhoff Type*

The RR Lyrae population of the M31 halo cannot be classified into either of the Oosterhoff (1939) types, but this is not because the various characteristics appear as an average of the two types (Figure 7). Looking at the ensemble variable population in Galactic globular clusters, the ratio of RRc to RRabc stars is 0.22 in Oosterhoff I clusters and 0.48 in Oosterhoff II clusters (Clement et al. 2001), while in the M31 halo it is 0.46 – a value in the Oosterhoff II regime. In contrast, looking at the mean period of the RRc stars in Galactic globular clusters, it is 0.326 days in Oosterhoff I clusters and 0.368 days in Oosterhoff II clusters (Clement et al. 2001), while in the M31 halo it is 0.316 days, within the Oosterhoff I regime. The mean period for the known RRab stars in Oosterhoff I clusters is 0.559 days, and in Oosterhoff II clusters it is 0.659 days (Clement et al. 2001), while in the M31 halo it is 0.594 days – midway between the two types. The RRab period distribution is more sharply peaked at this intermediate value than one might expect from an equal mix of Oosterhoff types (see Figure 8), but a Kolmogorov-Smirnov test shows the difference is not statistically significant. The period-amplitude diagram for the RRab stars is also suggestive of an intermediate Oosterhoff type (Figure 9). If we convert our $m_{F606W}$ amplitudes to $V$ amplitudes, and compare against the period-amplitude relations of Oosterhoff I and Oosterhoff II clusters (Clement 2000), the RRab stars in M31 fall between the two types, although there is a tendency toward Oosterhoff I at the larger amplitudes.

Although the Galactic halo field is more difficult to characterize than the Galactic clusters, it is interesting to note that the field RR Lyraes also show the Oosterhoff dichotomy, with a real gap in the distribution of period shifts at fixed amplitude with respect to the M3 RR Lyraes (see, e.g., Figure 8 of Suntzeff, Kinman, & Kraft 1991). However, these same data show that the Galactic field population is predominantly of Oosterhoff type I, as has been known for some time. In their study of the Palomar-Groningen Survey, Cacciari & Renzini (1976) found $<P_{ab}>= 0.529$ days, $<P_c>= 0.329$ days, and $N_c/N_{abc} = 0.09$. Selection effects in a field survey might favor RR Lyraes with higher amplitudes (thus reducing the relative number of RRc stars and long-period RRab stars), but these characteristics are all well within the Oosterhoff I regime. In contrast, the corresponding values for the M31 halo RR Lyraes are quite different. In particular, the mean RRab period is much longer in M31 ($<P_{ab}>= 0.594$ days), and the frequency of RRc variables is much higher ($N_c/N_{abc} = 0.46$). Most importantly, the distribution of period shifts of the M31 RR Lyraes with respect to the M3 RR Lyraes (i.e., the Oosterhoff I line in Figure 9) shows no such gap. All of these characteristics clearly distinguish the M31 halo field from the Milky Way halo field.

The characteristics of the M31 halo variables do not track those of the Local Group dSphs, either, except in the broad sense that the M31 halo cannot be put cleanly into one of the Oosterhoff types (Figure 7). For dSphs, the mean period of RRab stars tends to fall in the gap between Oosterhoff types

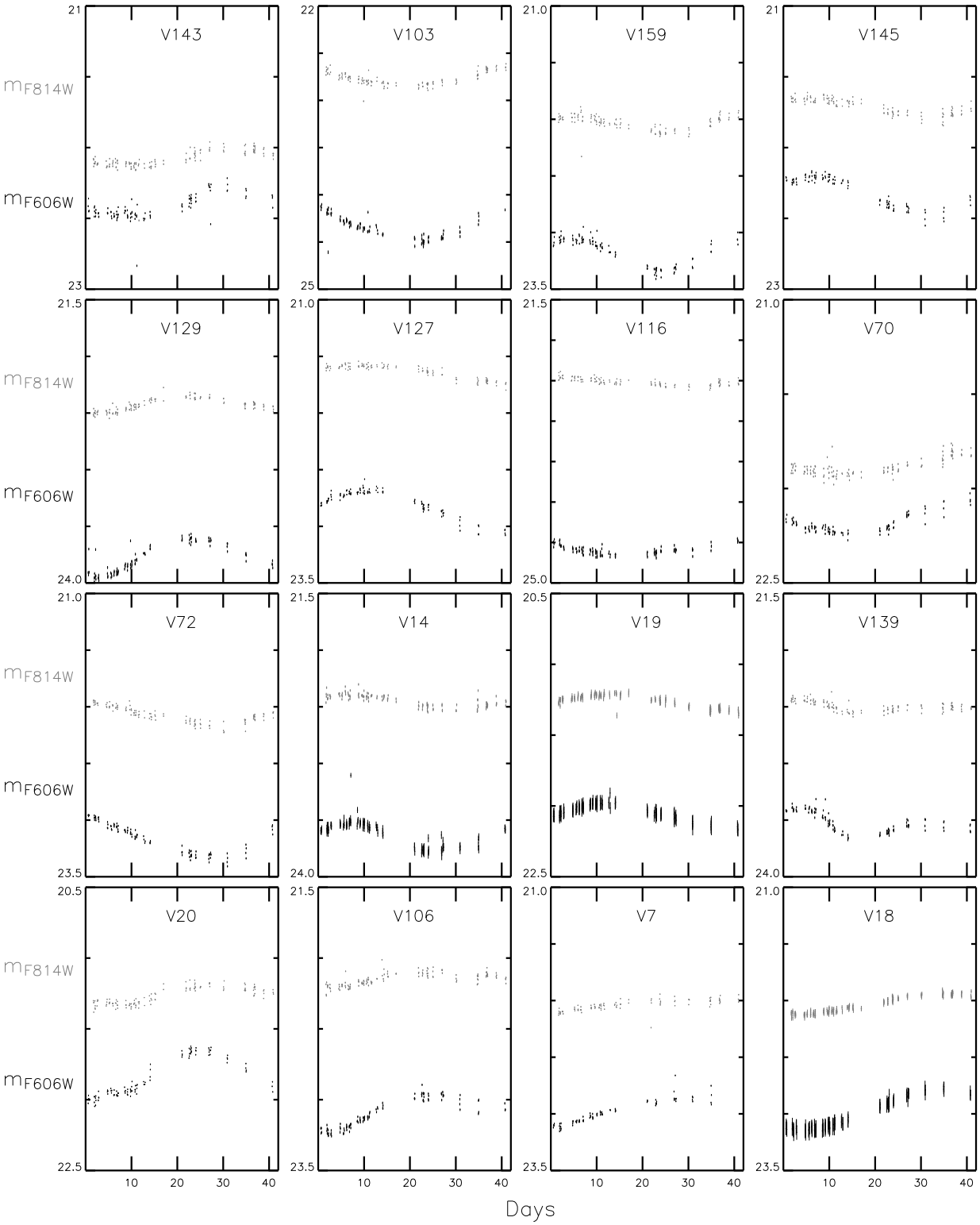


FIG. 4– The light curves for a subset of the bright LPVs and semiregulars in our field (those that varied by more than 0.1 mag in each bandpass), arranged roughly in order of increasing period (the 41 day span of our observations limits our ability to characterize the periods).

(Siegel & Majewski 2000; Pritzl et al. 2002, 2004; Dall'Ora et al. 2003 and references therein), as found in M31. However, the fraction of RR Lyrae stars that are RRc is higher in M31 (typical of Oosterhoff II) than that in any of the dSphs (which tend toward the Oosterhoff I values), while the mean period of RRc stars is much lower in M31 (typical of Oosterhoff I) than in any of the dSphs (which tend to fall in the gap between Oosterhoff types). These differences might suggest that the M31 halo is not comprised of dissolved globular clusters like those in the Milky Way, or dissolved Local Group dSphs. Note that globular clusters in the Large Magellanic Cloud are also predominantly of intermediate Oosterhoff type, in contrast to the clusters of the

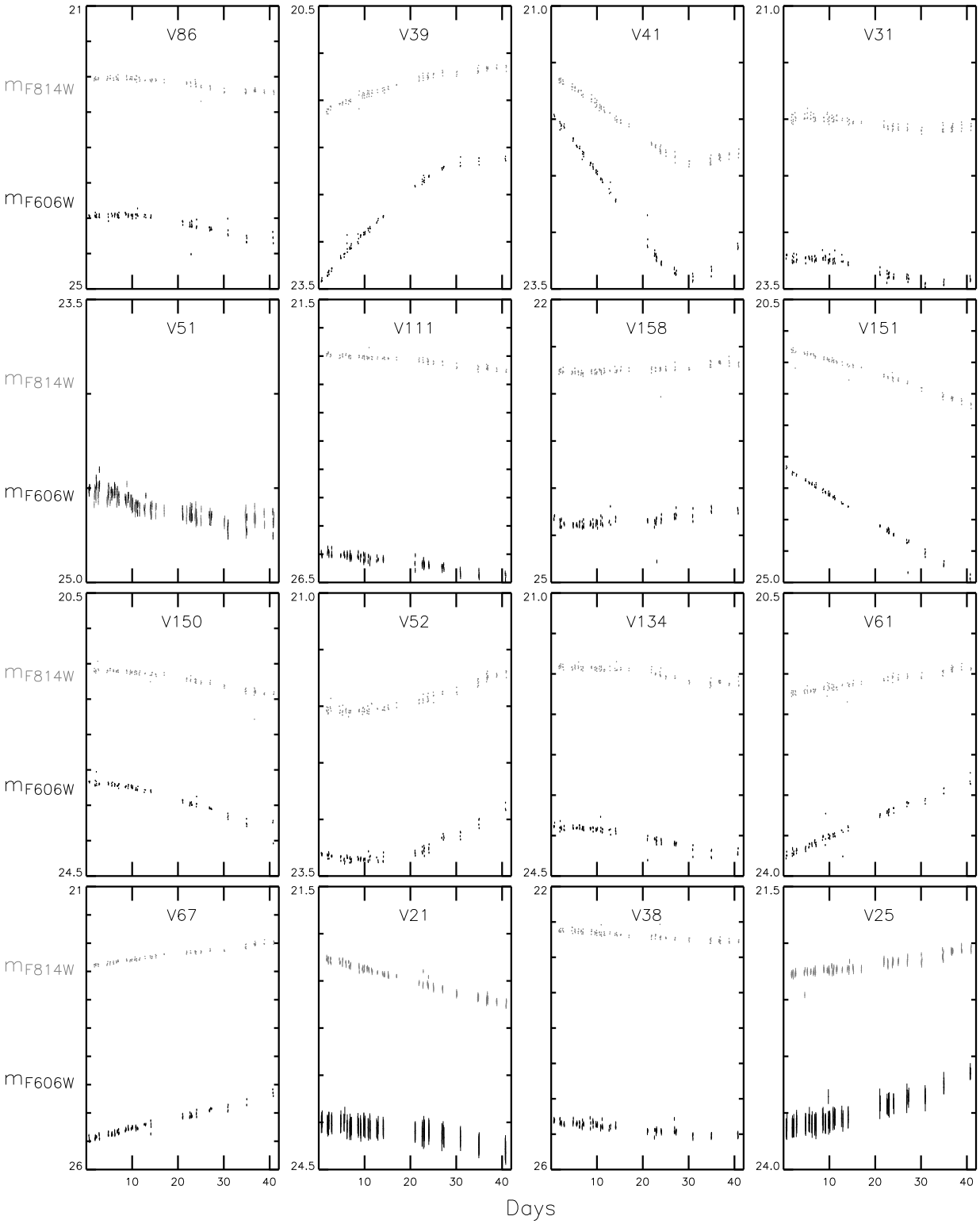


FIG. 4– Continued.

Milky Way (Bono, Caputo, & Stellingwerf 1994).

It has been argued that the Oosterhoff dichotomy among Galactic globular clusters is due to a real gap in metallicity between the two Oosterhoff types, with clusters at metallicities between the two Oosterhoff types having very blue HBs that do not populate the RR Lyrae instability strip (Renzini 1983; Sandage 1993). Local Group dSphs and LMC globular clusters fill the gap in a plot of [Fe/H] vs. $<P_{ab}>$, as illustrated by Siegel & Majewski (2000) and Pritzl et al. (2004) (see Figure 6 in each paper). This indicates that the dSphs and Galactic globular clusters occupy separate regions of the age vs. chemical composition parameter space (Renzini 1980), which in the simplest option reduces to the [Fe/H], age, and [$\alpha$/Fe] three-dimensional space. The M31 halo appears to bridge the gap in a manner similar to the dSphs, signaling that the early star formation history in the M31 halo proceeded at a different pace

TABLE 1
RR LYRAE PROPERTIES

| Name | R.A. (J2000) | Dec. (J2000) | Period (days) | $<m_{F606W}>$ (mag) | $<m_{F814W}>$ (mag) | $A_{F606W}$ (mag) | $A_{F814W}$ (mag) | class |
|---|---|---|---|---|---|---|---|---|
| V1 | $0^h45^m59.76^s$ | $40^o41'18.2''$ | 0.382 | 25.38 | 25.99 | 0.42 | 0.30 | c |
| V5 | $0^h46^m\ 0.61^s$ | $40^o40'52.4''$ | 0.339 | 25.55 | 26.17 | 0.40 | 0.29 | c |
| V8 | $0^h46^m\ 1.02^s$ | $40^o40'44.1''$ | 0.306 | 25.61 | 26.27 | 0.37 | 0.29 | c |
| V10 | $0^h46^m\ 0.68^s$ | $40^o41'\ 2.9''$ | 0.687 | 25.17 | 25.72 | 0.97 | 0.66 | ab |
| V11 | $0^h45^m56.88^s$ | $40^o43'44.1''$ | 0.331 | 25.64 | 26.25 | 0.40 | 0.28 | c |
| V27 | $0^h45^m57.64^s$ | $40^o43'33.5''$ | 0.287 | 25.65 | 26.32 | 0.49 | 0.32 | c |
| V28 | $0^h46^m\ 0.08^s$ | $40^o42'\ 2.9''$ | 0.532 | 25.59 | 26.15 | 0.85 | 0.70 | ab |
| V36 | $0^h46^m\ 2.04^s$ | $40^o41'29.0''$ | 0.627 | 25.32 | 25.91 | 1.06 | 0.73 | ab |
| V37 | $0^h46^m\ 3.26^s$ | $40^o40'39.9''$ | 0.301 | 25.48 | 26.17 | 0.46 | 0.33 | c |
| V40 | $0^h46^m\ 1.20^s$ | $40^o42'19.8''$ | 0.289 | 25.40 | 26.14 | 0.15 | 0.10 | c |
| V42 | $0^h46^m\ 0.77^s$ | $40^o43'\ 0.9''$ | 0.552 | 25.35 | 25.91 | 1.05 | 0.71 | ab |
| V43 | $0^h46^m\ 1.74^s$ | $40^o42'20.6''$ | 0.338 | 25.39 | 26.04 | 0.56 | 0.36 | c |
| V44 | $0^h45^m59.93^s$ | $40^o43'38.9''$ | 0.464 | 25.67 | 26.28 | 1.07 | 0.79 | ab |
| V47 | $0^h46^m\ 1.55^s$ | $40^o42'44.8''$ | 0.496 | 25.57 | 26.15 | 1.09 | 0.80 | ab |
| V50 | $0^h46^m\ 2.68^s$ | $40^o42'31.0''$ | 0.366 | 25.47 | 26.13 | 0.45 | 0.31 | c |
| V54 | $0^h46^m\ 4.33^s$ | $40^o41'35.2''$ | 0.366 | 25.42 | 26.05 | 0.38 | 0.26 | c |
| V57 | $0^h46^m\ 2.60^s$ | $40^o43'10.6''$ | 0.554 | 25.42 | 25.99 | 1.03 | 0.68 | ab |
| V59 | $0^h46^m\ 3.80^s$ | $40^o42'36.9''$ | 0.339 | 25.46 | 26.12 | 0.43 | 0.30 | c |
| V66 | $0^h46^m\ 4.71^s$ | $40^o42'32.6''$ | 0.714 | 25.37 | 25.87 | 0.51 | 0.39 | ab |
| V76 | $0^h46^m\ 5.86^s$ | $40^o42'52.9''$ | 0.274 | 25.42 | 26.14 | 0.15 | 0.11 | c |
| V77 | $0^h46^m\ 4.22^s$ | $40^o44'\ 5.8''$ | 0.678 | 25.52 | 26.04 | 0.63 | 0.43 | ab |
| V78 | $0^h46^m\ 8.34^s$ | $40^o41'24.6''$ | 0.774 | 25.38 | 25.92 | 0.49 | 0.42 | ab |
| V79 | $0^h46^m\ 4.60^s$ | $40^o44'\ 9.8''$ | 0.529 | 25.51 | 26.07 | 1.12 | 0.77 | ab |
| V80 | $0^h46^m\ 5.78^s$ | $40^o43'28.8''$ | 0.313 | 25.52 | 26.21 | 0.42 | 0.28 | c |
| V82 | $0^h46^m\ 5.29^s$ | $40^o44'\ 2.4''$ | 0.735 | 25.48 | 25.99 | 0.47 | 0.37 | ab |
| V83 | $0^h46^m\ 8.84^s$ | $40^o41'35.5''$ | 0.351 | 25.36 | 26.03 | 0.52 | 0.35 | c |
| V88 | $0^h46^m\ 9.86^s$ | $40^o41'\ 3.5''$ | 0.506 | 25.56 | 26.15 | 1.07 | 0.80 | ab |
| V89 | $0^h46^m\ 6.68^s$ | $40^o43'21.9''$ | 0.267 | 25.53 | 26.26 | 0.41 | 0.28 | c |
| V90 | $0^h46^m\ 7.71^s$ | $40^o42'51.1''$ | 0.353 | 25.49 | 26.11 | 0.50 | 0.26 | d |
| V95 | $0^h46^m\ 9.60^s$ | $40^o41'39.8''$ | 0.361 | 25.42 | 26.05 | 0.36 | 0.26 | c |
| V100 | $0^h46^m\ 6.94^s$ | $40^o43'58.7''$ | 0.275 | 25.59 | 26.29 | 0.48 | 0.35 | c |
| V102 | $0^h46^m\ 8.57^s$ | $40^o43'10.5''$ | 0.301 | 25.52 | 26.21 | 0.46 | 0.31 | c |
| V112 | $0^h46^m11.88^s$ | $40^o41'21.5''$ | 0.573 | 25.41 | 26.00 | 0.95 | 0.62 | ab |
| V114 | $0^h46^m10.11^s$ | $40^o42'54.5''$ | 0.726 | 25.30 | 25.80 | 0.33 | 0.24 | ab |
| V120 | $0^h46^m12.78^s$ | $40^o41'24.6''$ | 0.283 | 25.39 | 26.11 | 0.52 | 0.35 | c |
| V122 | $0^h46^m13.10^s$ | $40^o41'14.2''$ | 0.589 | 25.36 | 25.96 | 1.09 | 0.52 | ab |
| V123 | $0^h46^m12.46^s$ | $40^o41'42.2''$ | 0.631 | 25.27 | 25.82 | 0.67 | 0.50 | ab |
| V124 | $0^h46^m\ 9.88^s$ | $40^o43'34.7''$ | 0.627 | 25.35 | 25.89 | 0.75 | 0.52 | ab |
| V126 | $0^h46^m10.38^s$ | $40^o43'32.5''$ | 0.534 | 25.48 | 26.05 | 0.96 | 0.68 | ab |
| V130 | $0^h46^m11.91^s$ | $40^o42'45.1''$ | 0.263 | 25.66 | 26.37 | 0.48 | 0.33 | c |
| V131 | $0^h46^m13.72^s$ | $40^o41'30.6''$ | 0.327 | 25.50 | 26.15 | 0.38 | 0.22 | c |
| V133 | $0^h46^m13.43^s$ | $40^o41'54.5''$ | 0.572 | 25.37 | 25.95 | 0.88 | 0.64 | ab |
| V136 | $0^h46^m10.23^s$ | $40^o44'23.2''$ | 0.634 | 25.56 | 26.06 | 0.47 | 0.32 | ab |
| V137 | $0^h46^m11.13^s$ | $40^o43'48.8''$ | 0.280 | 25.60 | 26.27 | 0.34 | 0.22 | c |
| V140 | $0^h46^m14.51^s$ | $40^o41'37.0''$ | 0.559 | 25.38 | 25.96 | 1.12 | 0.84 | ab |
| V142 | $0^h46^m11.47^s$ | $40^o44'\ 4.1''$ | 0.554 | 25.41 | 25.97 | 0.91 | 0.65 | ab |
| V147 | $0^h46^m11.66^s$ | $40^o44'23.3''$ | 0.442 | 25.52 | 26.10 | 1.12 | 0.68 | ab |
| V157 | $0^h46^m16.21^s$ | $40^o41'47.6''$ | 0.329 | 25.47 | 26.16 | 0.40 | 0.29 | c |
| V160 | $0^h46^m14.30^s$ | $40^o43'22.7''$ | 0.611 | 25.26 | 25.81 | 0.68 | 0.53 | ab |
| V161 | $0^h46^m13.32^s$ | $40^o44'18.7''$ | 0.330 | 25.56 | 26.18 | 0.37 | 0.27 | c |
| V162 | $0^h46^m16.08^s$ | $40^o42'25.4''$ | 0.533 | 25.57 | 26.15 | 1.01 | 0.78 | ab |
| V163 | $0^h46^m15.92^s$ | $40^o42'37.9''$ | 0.313 | 25.35 | 26.00 | 0.37 | 0.25 | c |
| V164 | $0^h46^m14.21^s$ | $40^o43'55.8''$ | 0.580 | 25.45 | 26.01 | 0.85 | 0.64 | ab |
| V166 | $0^h46^m13.71^s$ | $40^o44'24.4''$ | 0.583 | 25.46 | 25.99 | 0.65 | 0.59 | ab |
| V167 | $0^h46^m10.38^s$ | $40^o43'44.0''$ | 0.621 | 25.43 | 25.95 | 0.67 | 0.47 | ab |

TABLE 2
RR LYRAE PHOTOMETRY[a]

| MJD | | Photometry (mag)[b] | | |
|---|---|---|---|---|
| (days) | Band | V1 | V5 | V8 |
| 52610.06377 | F606W | 25.58 | 25.75 | 25.87 |
| 52610.12537 | F606W | 25.27 | 25.57 | 25.57 |
| 52610.19249 | F606W | 99.99 | 25.42 | 25.48 |
| 52610.25919 | F606W | 25.22 | 25.44 | 25.51 |
| 52611.20557 | F814W | 26.09 | 26.14 | 26.39 |
| 52611.25942 | F814W | 25.98 | 26.07 | 99.99 |
| 52611.27610 | F814W | 25.96 | 26.09 | 26.47 |
| 52611.32653 | F814W | 25.75 | 26.19 | 26.37 |
| 52611.39623 | F606W | 25.29 | 25.74 | 25.42 |
| 52611.41250 | F606W | 25.37 | 25.83 | 25.47 |

[a]Table 2 is published in its entirety in the electronic edition of The Astronomical Journal. A portion is shown here for guidance regarding its form and content.
[b]A magnitude of 99.99 signifies missing data.

with respect to the Galactic halo, therefore resulting in different age vs. chemical composition patterns.

### 4.2. *Specific Frequency*

The specific frequency of RR Lyraes in the M31 halo has been the subject of debate, due perhaps in part to the difficulty of observing these stars from the ground. Pritchet & van den Bergh (1987) observed a $2.2' \times 3.3'$ field $40'$ from the nucleus on the southeast minor axis, and found 30 RR Lyraes with amplitudes $\gtrsim$0.7 mag. Assuming a completeness of 25%, they determined there should be 120 RR Lyraes with amplitudes $\gtrsim$0.7 mag. They took this to be a very strict lower limit, given the lack of low-amplitude RR Lyraes, and claimed their value was 55% of the frequency for M3 (NGC5272), a Galactic globular cluster with a high frequency of RR Lyraes. The specific frequency of RR Lyraes in M3, as given by Harris (1996) and normalized to a total cluster luminosity ($M_{Vt}$) of $-7.5$ mag, is $S_{RR} = N_{RR}10^{(M_{Vt}+7.5)/2.5} = 49$. Thus, Pritchet & van den Bergh (1987) determined $S_{RR} \approx 27$, which was a surprisingly high number, given the mean metallicity [Fe/H]$=-0.6$ of Mould & Kristian (1986).

Recently, Dolphin et al. (2003) observed a $9.6' \times 9.6'$ field that included the Pritchet & van den Bergh (1987) field, and found a much lower frequency of RR Lyraes. After finding 24 RR Lyraes and estimating a completeness of 24%, they estimated that there are 100 RR Lyraes in their field. Given the difference in field size, the Dolphin et al. (2003) frequency is 15 times smaller than that of Pritchet & van den Bergh (1987), i.e., $S_{RR} \approx 1.8$. Dolphin et al. (2003) claimed that their lower frequency was supported by the CMD of Brown et al. (2003) – the same data we are using in this paper – because they estimated that there were only 10 RR Lyraes in the Brown et al. (2003) data. However, the CMD shown by Brown et al. (2003) was displayed as a greyscale Hess diagram, in order to clearly show the characteristics of the main sequence turnoff in a catalog of $\sim 300,000$ stars; individual stars were not shown, nor was variability indicated in any way. In reality, 41 of the 55 RR Lyraes reported in our current work also appeared in the CMD of Brown et al. (2003); the remaining 14 were in the $\sim$ 20% of the image area masked for that earlier analysis of the star formation history (see §2).

These earlier estimates of the RR Lyrae frequency were limited by several factors. The first was uncertainty in the completeness. RR Lyraes were at the edge of detection in both the Dolphin et al. (2003) and Pritchet & van den Bergh (1987) studies, and neither group quantified the completeness at that depth through artificial star tests. Furthermore, the total luminosity in these fields could be estimated only from photographic plates or counts of the bright RGB stars. In contrast, our artificial star tests indicate that the completeness in our data

TABLE 3
POSITIONS OF OTHER VARIABLES

| Name | R.A. (J2000) | Dec. (J2000) | Name | R.A. (J2000) | Dec. (J2000) | Name | R.A. (J2000) | Dec. (J2000) |
|---|---|---|---|---|---|---|---|---|
| V6 | $0^h45^m57.91^s$ | $40^o42'48.1''$ | V64 | $0^h46^m\ 3.27^s$ | $40^o43'29.4''$ | V118 | $0^h46^m10.05^s$ | $40^o43'\ 6.0''$ |
| V7 | $0^h45^m58.14^s$ | $40^o42'38.6''$ | V65 | $0^h46^m\ 4.06^s$ | $40^o42'59.2''$ | V119 | $0^h46^m11.23^s$ | $40^o42'19.0''$ |
| V12 | $0^h45^m58.06^s$ | $40^o42'55.2''$ | V67 | $0^h46^m\ 4.42^s$ | $40^o42'46.9''$ | V127 | $0^h46^m11.02^s$ | $40^o43'\ 5.9''$ |
| V14 | $0^h45^m58.78^s$ | $40^o42'29.7''$ | V70 | $0^h46^m\ 3.88^s$ | $40^o43'28.5''$ | V128 | $0^h46^m12.17^s$ | $40^o42'18.4''$ |
| V18 | $0^h45^m58.87^s$ | $40^o42'32.3''$ | V72 | $0^h46^m\ 6.25^s$ | $40^o41'53.8''$ | V129 | $0^h46^m\ 9.88^s$ | $40^o43'57.4''$ |
| V19 | $0^h45^m58.90^s$ | $40^o42'30.9''$ | V74 | $0^h46^m\ 4.44^s$ | $40^o43'25.7''$ | V134 | $0^h46^m13.50^s$ | $40^o41'53.2''$ |
| V20 | $0^h46^m\ 1.02^s$ | $40^o41'\ 2.1''$ | V84 | $0^h46^m\ 5.30^s$ | $40^o44'\ 5.8''$ | V139 | $0^h46^m11.90^s$ | $40^o43'17.9''$ |
| V21 | $0^h45^m58.90^s$ | $40^o42'32.7''$ | V85 | $0^h46^m\ 9.12^s$ | $40^o41'24.7''$ | V143 | $0^h46^m14.94^s$ | $40^o41'42.8''$ |
| V25 | $0^h45^m58.97^s$ | $40^o42'32.0''$ | V86 | $0^h46^m\ 9.55^s$ | $40^o41'\ 8.5''$ | V145 | $0^h46^m14.38^s$ | $40^o42'13.8''$ |
| V29 | $0^h46^m\ 1.76^s$ | $40^o40'53.1''$ | V91 | $0^h46^m\ 7.74^s$ | $40^o42'50.6''$ | V150 | $0^h46^m12.63^s$ | $40^o43'48.2''$ |
| V31 | $0^h46^m\ 2.46^s$ | $40^o40'41.3''$ | V93 | $0^h46^m\ 9.40^s$ | $40^o41'45.2''$ | V151 | $0^h46^m13.16^s$ | $40^o43'36.0''$ |
| V38 | $0^h46^m\ 1.79^s$ | $40^o41'44.0''$ | V94 | $0^h46^m\ 9.77^s$ | $40^o41'29.9''$ | V158 | $0^h46^m13.67^s$ | $40^o43'37.6''$ |
| V39 | $0^h46^m\ 0.08^s$ | $40^o42'57.0''$ | V99 | $0^h46^m\ 6.54^s$ | $40^o44'\ 8.0''$ | V159 | $0^h46^m14.91^s$ | $40^o42'51.6''$ |
| V41 | $0^h46^m\ 1.07^s$ | $40^o42'44.9''$ | V103 | $0^h46^m\ 8.70^s$ | $40^o43'10.2''$ | V168 | $0^h46^m\ 0.63^s$ | $40^o41'13.8''$ |
| V48 | $0^h46^m\ 2.27^s$ | $40^o42'16.3''$ | V105 | $0^h46^m\ 9.32^s$ | $40^o42'53.2''$ | V169 | $0^h46^m\ 2.52^s$ | $40^o40'37.7''$ |
| V51 | $0^h46^m\ 1.59^s$ | $40^o43'18.1''$ | V106 | $0^h46^m10.84^s$ | $40^o41'51.5''$ | V170 | $0^h46^m\ 8.72^s$ | $40^o41'53.0''$ |
| V52 | $0^h46^m\ 2.51^s$ | $40^o42'39.2''$ | V111 | $0^h46^m11.28^s$ | $40^o41'42.7''$ | V171 | $0^h46^m\ 7.35^s$ | $40^o44'17.1''$ |
| V60 | $0^h46^m\ 4.91^s$ | $40^o41'55.9''$ | V113 | $0^h46^m\ 8.95^s$ | $40^o43'29.5''$ | V172 | $0^h46^m\ 9.93^s$ | $40^o43'18.3''$ |
| V61 | $0^h46^m\ 5.72^s$ | $40^o41'24.2''$ | V116 | $0^h46^m12.44^s$ | $40^o41'20.8''$ | V173 | $0^h46^m10.45^s$ | $40^o43'\ 1.6''$ |
| V63 | $0^h46^m\ 5.43^s$ | $40^o41'55.9''$ | V117 | $0^h46^m11.67^s$ | $40^o41'54.6''$ | V174 | $0^h46^m\ 8.98^s$ | $40^o43'\ 9.2''$ |

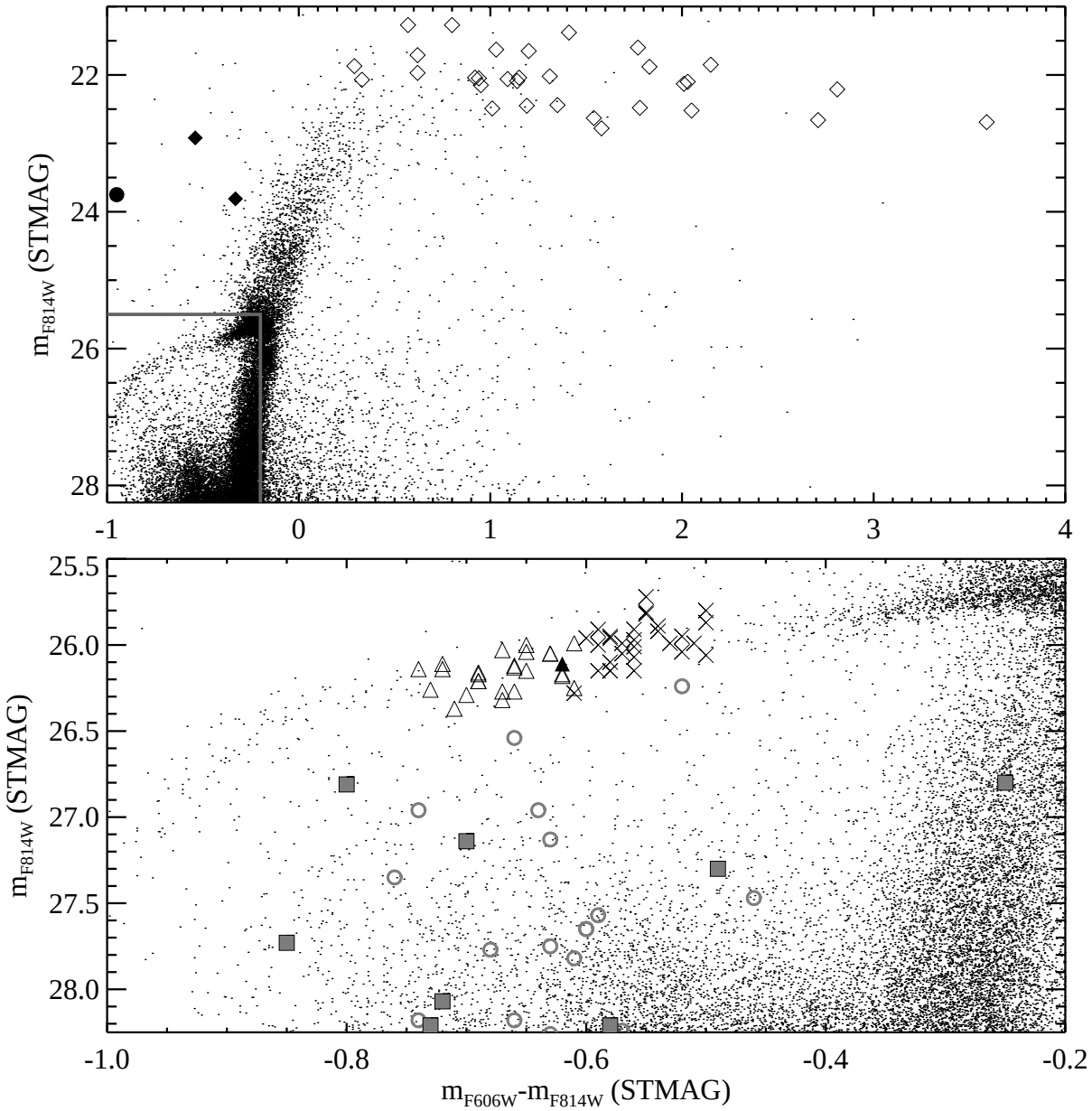


FIG. 5– *Top panel:* Subset of the M31 halo CMD of Brown et al. (2003), highlighting the bright variables. From Figure 2, V84 is marked by a closed circle, while V118 and V60 are marked by closed diamonds. The variables of Figure 4 are shown by open diamonds. *Bottom panel:* Expanded view of the faint variables: RRab stars (*crosses*), RRc stars (*open triangles*), an RRd star (*closed triangle*), dwarf Cepheids (*open circles*), and eclipsing binaries (*closed squares*).

is ≈100% at the horizontal branch, our time sampling enables a search for periodicity with high statistical significance, and our deep catalog allows an accurate determination of the total luminosity in our field. Brown et al. (2003) determined $\mu_V \approx 26.3$ mag arcsec$^{-2}$ in this field. Assuming an extinction of $E(B-V) = 0.08 \pm 0.03$ mag (Schlegel et al. 1998) and a distance modulus $(m-M)_0 = 24.44 \pm 0.1$ mag (Freedman & Madore 1990), we estimate a total brightness in our field of $M_V \approx -10.0$ mag, and $S_{RR} \approx 5.6$ ($\sim$ 1 RR Lyrae star per $1.5 \times 10^4 L_\odot$). Our frequency is $\sim$3 times higher than that found by Dolphin et al. (2003), with the number of RR Lyraes compared either to the number of RGB stars (the metric of Dolphin et al. 2003) or the total luminosity of the field (the metric of Harris 1996). The specific frequency we find is much higher than one would expect for a population with metallicity [Fe/H]$= -0.8$ (Figure 10), but not surprising given that the M31 halo has a wide metallicity distribution, with $\sim$40% of the stars at $-2.5 <$[Fe/H]$< -1$ (Durrell et al. 2001). Because about half of the M31 halo is metal-rich and of intermediate age (Brown et al. 2003), and thus incapable of producing RR Lyrae stars, one could reasonably shift the location of the M31 data point in Figure 10 to a metallicity near [Fe/H]$= -1.6$ and to a frequency twice as large as that found at [Fe$/$H$] = -0.8$.

### 4.3. *Metallicity*

Given a larger number of RR Lyraes than expected for a mean metallicity of [Fe/H]$= -0.8$, it is reasonable to assume that the RR Lyraes come from the old, metal-poor component of the M31 halo. As done in studies of dSph populations (e.g., Pritzl et al. 2002; Siegel & Majewski 2000), we can use one of several empirical relations to estimate the metallicity of the RR Lyraes in our field. Looking at the mean properties of the

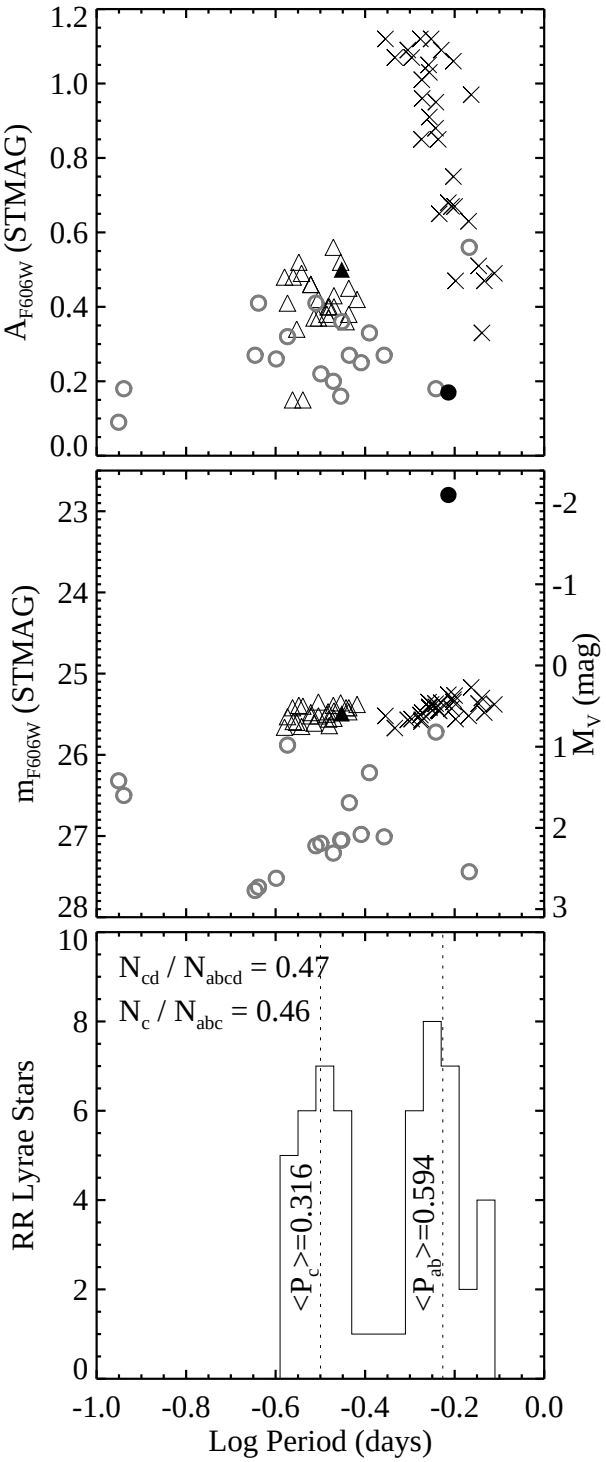


FIG. 6– *Top panel:* The amplitude vs. period diagram for short period variables (excluding the eclipsing binaries). The RRab stars (*crosses*) are well-separated from the RRc stars (*open triangles*), but the dwarf Cepheids (*open circles*) are mixed in with the RR Lyraes. The RRd star (*closed triangle*) is mixed in the main RRc clump. The bright blue variable above the HB is also marked (*closed circle*). *Middle panel:* The luminosity vs. period diagram, with the same symbols. The RR Lyraes are well-separated from the other variables, although two "dwarf Cepheids" might actually be RR Lyraes. The left axis provides the observed F606W magnitudes, while the right gives the transformation to $M_V$ appropriate for the color of the center of the RR Lyrae gap, assuming the Cepheid distance to M31 (see §4.6 for details). *Bottom panel:* The period histogram for the RR Lyraes. The parameters used to distinguish Oosterhoff type are labeled.

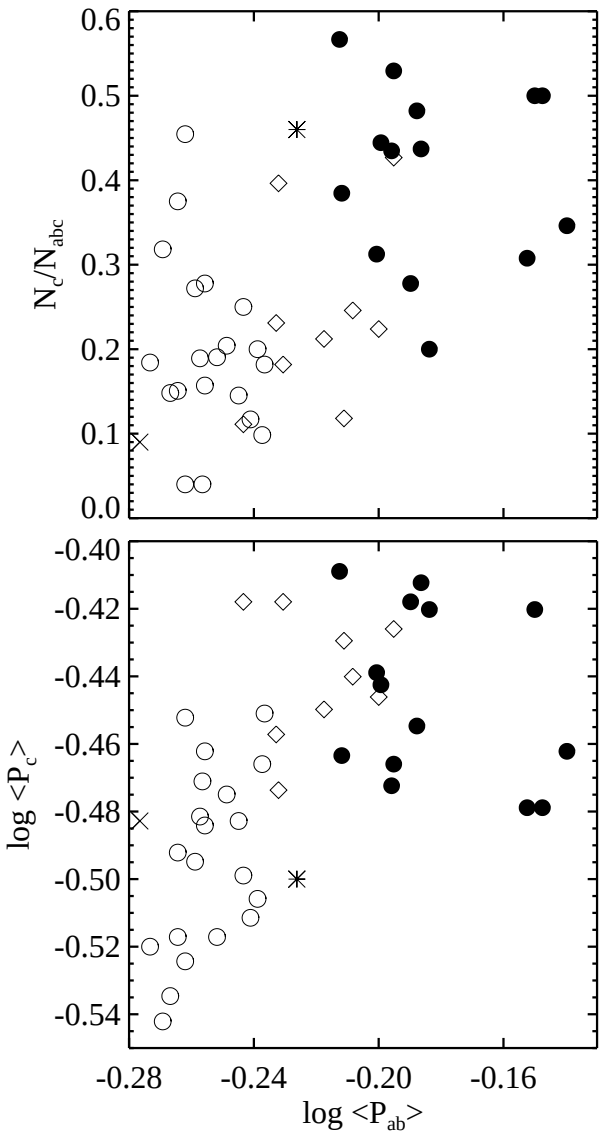


FIG. 7– *Top panel:* The fractions of RRab+RRc stars that are RRc, vs. the mean RRab periods, for different populations. Galactic globular clusters (Clement et al. 2001) of Oosterhoff I (*open circles*) and Oosterhoff II (*closed circles*) types are well separated, while Local Group dSphs (*diamonds*; Pritzl et al. 2002, 2004; Dall'Ora et al. 2003) and the M31 halo (*asterisk*) bridge the gap; the Milky Way halo field is, on average, Oosterhoff I (*cross*; Cacciari & Renzini 1976). The fraction of RRc stars in the M31 halo is like that in Oosterhoff II clusters, while the fraction of RRc stars in dSphs is like that in Oosterhoff I clusters. *Bottom panel:* The mean RRc period vs. the mean RRab period. Again, the dSphs and the M31 halo bridge the gap between Oosterhoff types, but the mean RRc period in M31 is like that in Oosterhoff I clusters, while the mean RRc period in dSphs is like that in Oosterhoff II clusters.

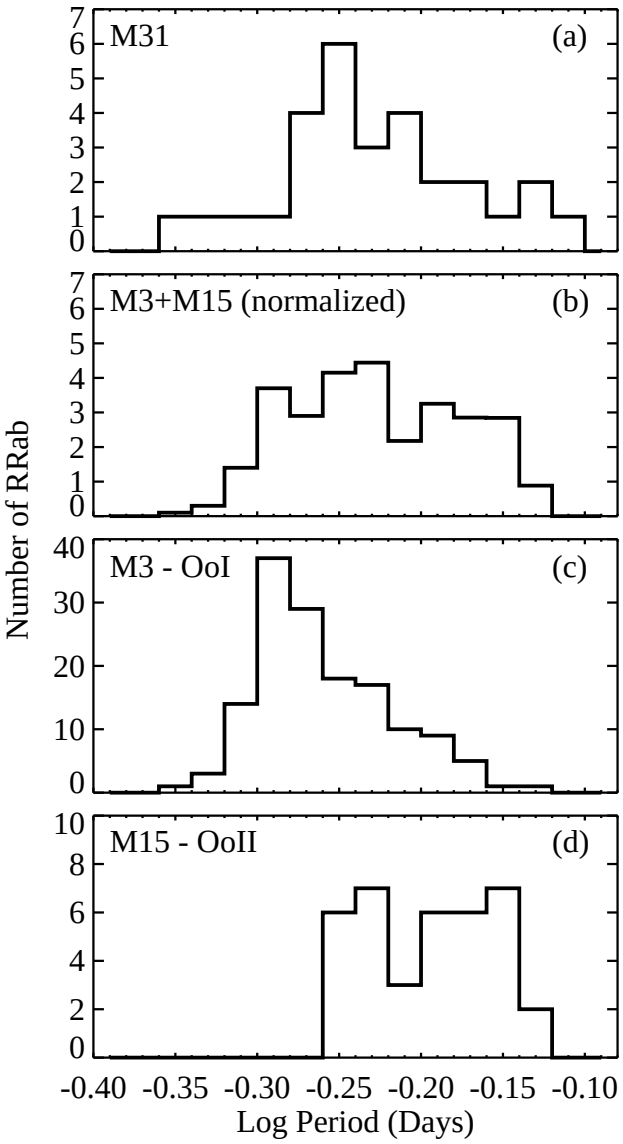


FIG. 8– *Panel (a):* The period distribution of RRab stars in the M31 halo. *Panel (b):* The period distribution of RRab stars when the stars are drawn equally from M3 and M15 – two clusters rich in RR Lyraes with distinct Oosterhoff types. *Panel (c):* The period distribution in M3 (Clement et al. 2001). *Panel (d):* The period distribution in M15 (Clement et al. 2001).

RRab and RRc stars, the period-metallicity relations of Sandage (1993) give [Fe/H] = (–log$<P_{ab}>$ $-0.389)/0.092 = -1.77$, and [Fe/H] = (–log$<P_c>$ $-0.670)/0.119 = -1.43$, on the Zinn & West (1984) scale. Given the ensemble population in the M31 halo and the scatter for these relations shown by Sandage (1993), the difference in metallicity for the RRab and RRc stars is not significant, but we can say that the RR Lyraes lie in the metal-poor tail of the halo metallicity distribution. This finding is further supported by the period-amplitude-metallicity relation of Alcock et al. (2000), which provides metallicities on the Zinn & West (1984) scale for individual RRab stars: [Fe/H]= –8.85(log$P_{ab} + 0.15A_V$)–2.60. Converting our amplitudes in the $m_{F606W}$ bandpass to those in Johnson $V$, we find a mean [Fe/H] of –1.79, with a standard deviation of 0.32; the accuracy of this method is $\sigma_{[\mathrm{Fe/H}]} = 0.31$ per star (Alcock et al. 2000), so the dispersion in our individual metallicities is not statistically significant.

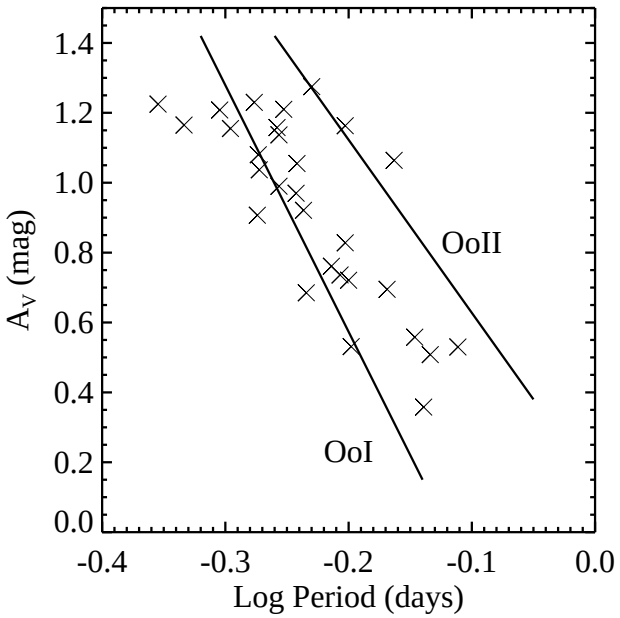


FIG. 9– The period-amplitude diagram for the RRab stars of the M31 halo (*crosses*), compared to the period-amplitude relations for Oosterhoff I and Oosterhoff II clusters (*lines*; Clement 2000). Note that we converted amplitudes in the $m_{F606W}$ bandpass to amplitudes in Johnson $V$ using Lejeune synthetic spectra, but this correction is small (a 6–10% increase in the F606W amplitude). The M31 halo stars appear to be an intermediate case between Oosterhoff types, although there is a tendency toward the Oosterhoff I type at large amplitudes.

### 4.4. *Double-Mode Pulsators*

As mentioned in §2, five RR Lyrae stars in our sample show significant scatter in their light curves, as expected for double-mode pulsators (RRd stars) and RRab stars exhibiting the Blazhko effect. One of these stars, V90, shows clear periodicity at two different periods, with $P_0 = 0.4735$ days and $P_1 = 0.3534$ days. The ratio $P_1/P_0$ is sensitive to the mass of the RRd star, with RRd stars from the two Oosterhoff types clearly separated in a $P_1/P_0$ vs $P_0$ diagram (see Bono et al. 1996 and references therein). Using these periods to place our confirmed RRd star in the diagrams of Bono et al. (1996), we find that the $P_0$ for this star is similar to that of RRd stars found in Oosterhoff I clusters, but the $P_1/P_0$ ratio is typical for RRd stars found in Oosterhoff II clusters, with a mass of $\approx 0.75\ M_\odot$. It is curious that an individual star in the M31 halo cannot be placed into either Oosterhoff type in such a diagram; again, this suggests that the M31 halo population is not a simple mix of Oosterhoff types.

### 4.5. *Distance*

With the metallicities derived above, we can estimate the distance to the M31 halo population using the relation of Carretta et al. (2000): $M_V = (0.18 \pm 0.09)([\mathrm{Fe/H}] + 1.5) + (0.57 \pm 0.07)$. Note that this relation is consistent with the average of the methods discussed by Cacciari & Clementini (2003), who give an excellent review of distance determination using RR Lyrae stars. Using the synthetic spectra of Lejeune et al. (1997), an assumed extinction of $E(B-V) = 0.08 \pm 0.03$ (Schlegel et al. 1998), and the extinction curve of Fitzpatrick (1999), we can calculate the offset between $m_{F606W}$ and $V$ as a function of $m_{F606W} - m_{F814W}$. The RRab stars have a color range $-0.61 \leq (m_{F606W} - m_{F814W}) \leq -0.5$ mag, with corresponding corrections of $-0.17 \leq (V - m_{F606W}) \leq -0.13$ mag; the

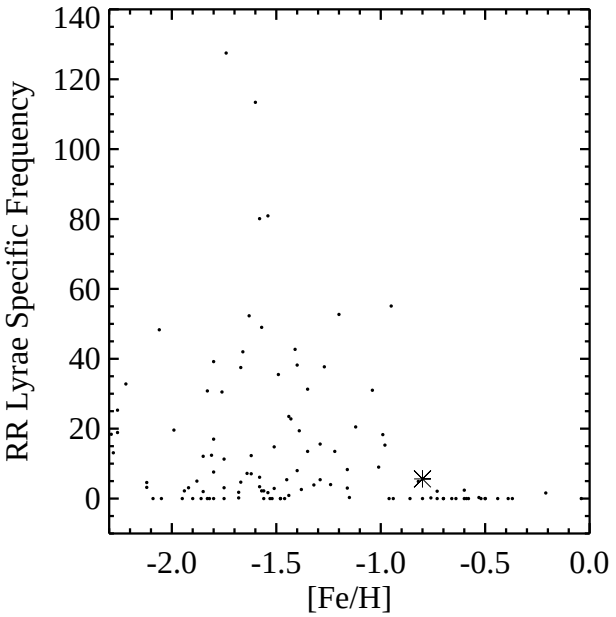


FIG. 10– The specific frequency of RR Lyraes, normalized to a population at $M_{Vt} = -7.5$ mag, as a function of metallicity, for Galactic globular clusters (*points*; Harris 1996) and the M31 halo (*asterisk*). Although the frequency of RR Lyraes in the M31 halo is higher than expected for the mean halo metallicity, the RR Lyraes have a metallicity near [Fe/H]$= -1.6$. Considered as part of the old metal-poor population, the frequency in the M31 halo is not surprising.

RRc stars have a color range $-0.74 \leq (m_{F606W} - m_{F814W}) \leq -0.61$ mag, with corresponding corrections of $-0.21 \leq (V - m_{F606W}) \leq -0.17$ mag. After correcting the individual stars with the offsets appropriate to their colors, the RRab stars lie at $<m_{F606W}> = 25.43$ mag and $<V> = 25.28 \pm 0.01$ mag, while the RRc stars lie at $<m_{F606W}> = 25.49$ mag and $<V> = 25.31 \pm 0.01$ mag (the statistical errors on $<V>$ are much smaller than 0.01 mag, but the throughputs of the ACS filters are only known to $\sim$1%). Assuming [Fe/H]$= -1.77$, the Carretta et al. (2000) relation yields $M_V = 0.52 \pm 0.07$ mag for the RRab stars; assuming [Fe/H]$= -1.43$ gives $M_V = 0.58 \pm 0.07$ mag for the RRc stars. With an extinction of $A_V = 0.25 \pm 0.09$, we have distance moduli of $(m-M)_0 = 24.51 \pm 0.11$ mag for the RRab stars, and $(m-M)_0 = 24.48 \pm 0.11$ mag for the RRc stars. Averaging these results gives an RR Lyrae distance modulus of $(m-M)_0 = 24.5 \pm 0.1$ mag, which is in very good agreement with the Cepheid distance modulus of $(m-M)_0 = 24.44 \pm 0.1$ mag (Freedman & Madore 1990), given the uncertainties.

Dolphin et al. (2003) made similar estimates of the RR Lyrae luminosity in their field, but found $<V_0> = 24.81 \pm 0.11$ mag – about 0.24 mag brighter than our own estimate. Given their relatively low completeness, it is plausible that their RR Lyrae sample is biased toward brighter stars (although they argue otherwise). Dolphin inspected the Brown et al. (2003) CMD and found support for their bright RR Lyrae estimate, but we stress again that our previous presentation of the M31 halo data only showed a greyscale Hess diagram, making such estimates from the published figure difficult.

## 5. OTHER VARIABLES

Although the focus of this paper is the RR Lyrae population in the Andromeda halo, we briefly note the other classes of variables suitable for followup studies. The short period variables below the HB (see Figures 2 and 5) fall in the broad category of dwarf Cepheids; given the wide age range in the M31 halo (Brown et al. 2003), these are probably a mix of pulsating and eclipsing stars on the main sequence (e.g., $\delta$ Scuti stars) and in the blue straggler population (e.g., SX Phoenicis stars). Above the HB, the bluest star (V84) is outside of the Cepheid instability strip, but might be a pulsating post-asymptotic branch star. The other two stars above the HB (V118 and V60) have periods that are longer than typically found for Anomalous Cepheids, but their luminosities and periods put them close to the Population I and Population II Cepheids. In any case, if they are both pulsating variables, they cannot belong to the same class, given that the star with the longer period is fainter. The semiregulars and long period variables (see Figure 4) include RV Tauri stars and Mira stars. In globular clusters, Miras are found only at [Fe/H] $> -1$ (Frogel & Whitelock 1998), where they have periods $\lesssim 310$ days. Given the wide age spread in the M31 halo, one might expect some of the Miras to have periods longer than 310 days, but characterization of these stars would require a longer baseline than that currently available.

## 6. SUMMARY

We have presented a complete survey of the RR Lyrae stars in an M31 halo field, 51 arcmin from the nucleus. We find 29 RRab stars with a mean period of 0.594 days, 25 RRc stars with a mean period of 0.316 days, and 1 RRd star with a fundamental period of 0.473 days and a first overtone period of 0.353 days. The RR Lyrae population of the M31 halo cannot be clearly placed into either Oosterhoff type, and is distinct from the Milky Way cluster and halo field populations. In a broad sense, the Local Group dSphs share the intermediate Oosterhoff status found the M31 halo, but the characteristics of the M31 RR Lyraes ($<P_{ab}>$, $<P_c>$, $N_c/N_{abc}$) are distinct from the dSphs, suggesting that the M31 halo is not comprised of dissolved globular clusters like those in the Milky Way or dissolved Local Group dSphs. The specific frequency of RR Lyraes ($S_{RR} = 5.6$) is very high for a mean halo metallicity of [Fe/H]$= -0.8$, but within the normal range when considered as a component of the old, metal-poor halo population. The mean metallicity of the RR Lyrae population is indeed much lower than that of the halo, with a mean [Fe/H]$= -1.77$ for the RRab stars and a mean [Fe/H]$= -1.43$ for the RRc stars. The distance to M31 determined from the RR Lyrae luminosity is $(m-M)_o = 24.5 \pm 0.1$ mag, in good agreement with the Cepheid distance.

Support for proposal 9453 was provided by NASA through a grant from STScI, which is operated by AURA, Inc., under NASA contract NAS 5-26555. We are grateful to P. Stetson for providing the latest version of DAOPHOT and assistance with its use, and to R. Gilliland for useful discussions. H. Smith kindly reviewed a draft of this manuscript and offered helpful comments. We thank the members of the scheduling and operations teams at STScI (especially P. Royle, D. Taylor, and D. Soderblom) for their efforts in executing a large program during a busy HST cycle. Our paper was improved by the suggestions of an anonymous referee.

REFERENCES

Alcock, C., et al. 2000, AJ, 119, 2194
Bono, G., Caputo, F., Castellani, V., & Marconi, M. 1996, ApJ, 471, 33
Bono, G., Caputo, F., & Stellingwerf, R.F. 1994, ApJ, 423, 294
Brown, T.M. 2003, in "The Local Group as an Astrophysical Laboratory," ed. M. Livio (Cambridge University Press), in press, astro-ph/0308298.
Brown, T.M., Ferguson, H.C., Smith, E., Kimble, R.A., Sweigart, A.V., Renzini, A., Rich, R.M., & VandenBerg, D.A. 2003, ApJ, 592, L17.
Cacciari, C., & Clementini, G. 2003, in Lecture Notes in Physics Volume 635, Stellar Candles for the Extragalactic Distance Scale, ed. D.M. Alloin & W. Gieren (New York: Springer), 635, 105
Cacciari, C., & Renzini, A. 1976, A&AS, 25, 303
Carretta, E., Gratton, R.G., Clementini, G., Fusi Pecci, F. 2000, 533, 215
Clement, C.M. 2000, in ASP Conf. Ser. 203, The Impact of Large-Scale Surveys on Pulsating Star Research, ed. L. Szabados & D.W. Kurtz (IAU Colloq. 176) (San Francisco: ASP), 266
Clement, C.M., et al. 2001, AJ, 122, 2587
Dall'Ora, M., et al. 2003, AJ, 126, 197
Dolphin, A.E., Saha, A., Olszewski, E.W., Thim, F. Skillman, E.D., Gallagher, J.S., & Hoessel, J. 2003, AJ, in press, astro-ph/0311300
Durrell, P.R., Harris, W.E., & Pritchet, C.J. 2001, AJ, 121, 2557
Ferguson, A.M.N., Irwin, M.J., Ibata, R.A., Lewis, G.F., & Tanvir, N.R. 2002, AJ, 124, 1452
Fitzpatrick, E.L. 1999, PASP, 111, 63
Ford, H.C., et al. 1998, Proc. SPIE, 3356, 234.
Freedman, W.L., & Madore, B.F. 1990, ApJ, 365, 186
Frogel, J.A., & Whitelock, P.A. 1998, 116, 754
Harris, W.E. 1996, AJ, 112, 1487
Holland, S., Fahlman, G.G., & Richer, H.B. 1997, AJ, 114, 1488
Krist, J. 1995, ASP Conference Series 77, Astronomical Data Analysis Software and Systems IV, ed. R.A. Shaw, H.E. Payne, & J.J.E. Hayes, 349
Lafler, J., & Kinman, T.D. 1965, ApJS, 11, 216
Lejeune, T., Cuisinier, F., & Buser, R. 1997, A&AS, 125, 229
Lomb, N.R. 1976, Ap&SS
Mateo, M. 1998, ARA&A, 36, 435
Mould, J., & Kristian, J. 1986, ApJ, 305, 591
Oosterhoff, P. Th. 1939, Observatory, 62, 104
Press, W.H., & Rybicki, G.B. 1989, ApJ, 338, 277
Pritchet, C.J., & van den Bergh, S. 1987, ApJ, 316, 517
Pritzl, B.J., Armandroff, T.E., Jacoby, G.H., & Da Costa, G.S. 2002, AJ, 124, 1464
Pritzl, B.J., Armandroff, T.E., Jacoby, G.H., & Da Costa, G.S. 2002, AJ, 127, 318
Renzini, A. 1980, Mem. S. A. It., 51, 749
Renzini, A. 1983, Mem. S. A. It., 54, 335
Ryan, S.G., & Norris, J.E. 1991, AJ, 101, 1865
Sandage, A. 1993, AJ, 106, 687
Sargent, W.L.W., Kowal, C.T., Hartwick, F.D.A., van den Bergh, S. 1977, AJ, 82, 947
Scargle, J.D. 1982, ApJ, 263, 835
Schlegel, D.J., Finkbeiner, D.P., & Davis, M. 1998, ApJ, 500, 525
Siegel, M.H., & Majewski, S.R. 2000, AJ, 120, 284
Smith, H.A., et al. 2003, PASP, 115, 43
Stetson, P. 1987, PASP, 99, 191
Suntzeff, N.B., Kinman, T.D., & Kraft, R.B. 1991, ApJ, 367, 528
van den Bergh, S. 1999, A&A Rev., 9, 273
VandenBerg, D.A., 2000, ApJS, 129, 315
Zinn, R., & West, M.J. 1984, ApJS, 55, 45